Multivariable fuzzy inference system for fingerprinting indoor localization

Oussalah, M.; Alakhras, M.; Hussein, M.i.

Accepted Manuscript

Multivariable fuzzy inference system for fingerprinting indoor localization

M. Oussalah, M. Alakhras, M. Hussein

Please cite this article in press as: M. Oussalah et al., Multivariable fuzzy inference system for fingerprinting indoor localization, *Fuzzy Sets and Systems* (2014), http://dx.doi.org/10.1016/j.fss.2014.08.001

Multivariable Fuzzy Inference System For Fingerprinting Indoor Localization

M. Oussalah
University of Birmingham
EECE, UK

M.Oussalah@bham.ac.uk

M Alakhras

United Arab Emirate University,
UAE

alakhras@uaeu.ac.ae

M. Hussein

United Arab Emirate
University, UAE

COE, mihussein@uaeu.ac.ae

University   of   Birmingham,
EECE UK, mxa915@bham.ac.uk

Abstract—**The emergence of wireless sensor network as has raised the need for cheap wireless indoor localization technique This paper considers the problem of fingerprinting indoor localization based on signal strength measurements RSS. A new approach based on Fuzzy logic has been put forward. The proposal makes use of k-nearest neighbor classification in signal space. The localization of target node is then determined as a weighted combination of nearest fingerprints. The weights are determined using Takagi-Sugeno fuzzy controller with two inputs. A new enhancement of K-nearest neighbor based on triangular area measurements to outlier some miss elected neighbors has been proposed to enhance the accuracy of location estimation. The performances of the developed estimation algorithm have been evaluated using both Monte Carlo simulations and real testbed scenarios while compared to other alternative approaches.**

I.   INTRODUCTION

Localization techniques gained potential attention from various disciplines ranging from pure engineering where the issue of identifying critical imperfections in the system design is of paramount interest, to social and/or psychological domain where detection of community syllabus or relevant individual behavior plays key role in enhancing cohesion and prospect of a whole society. Development of robotics platforms has also raised the importance of the localization due to its criticality to subsequent tasks like navigation, environment mapping and path planning [1] in the sense that the integration of sensorial information would typically require the positioning information. This is particularly highlighted in applications related to hazardous environments like space and deep ocean explorations, nuclear facility inspections as well as medical interventions, e.g., surgical operations, endoscopic analysis, among others, where failure of localization task has caused major consequences [2,3]. On the other hand, the emergence and proliferation of the wireless communication industry and the popularity of mobile and handheld devices with billions of users has also prompted the interest in the localization task to a higher level where the location of the data is as important as the data itself. This is referred to as Location Based Services (LBS), where the quality of service (QoS) received is highly dependent on the accuracy of the location estimation [4]. As shown in Fig 1, localization techniques establish the core backbone of LBS systems in a variety of contexts. For instance, the nearest printer/scanner may be selected to print/scan user's documents; the access rights to secured files maybe grunted according to employee's office location in the enterprise [5]. Localization is also a key in ubiquitous computing architectures as sensors are distributed across the whole environment such as intelligent cities and health monitoring. Mobile services such as user's tracking, location specific advertising, finding the nearest points of interest, route planner, among others, were put forward. In this respect, the LBS makes use of technologies involving Global Positioning System (GPS), GSM for outdoor environments, and local range technologies, e.g., Bluetooth, WiFi, Radio Frequency Identification (RFID) [6].

Although it is acknowledged that the Global Positioning Systems (GPS) technology becomes effective and affordable in open and flat outdoor environments, its use in Wireless Local Area Network (WLAN) indoor environments as well as in Non-Light-Of-Sight (NLOS) scenarios is not effective. This triggers the need for alternative localization techniques in wireless systems. Besides, the constraints imposed by regulator bodies to force the operators to achieve minimal positioning accuracy regardless of availability of GPS data for emergency purpose, together with the need to accommodate local network constraints, e.g., communication cost and nature of outcome, pushed towards the development of wireless like solution as a pre-requisite to the

success of the underlying application (s). Such solutions may also integrate GPS data if available as in Assisted GPS-WiFi like approach [4].
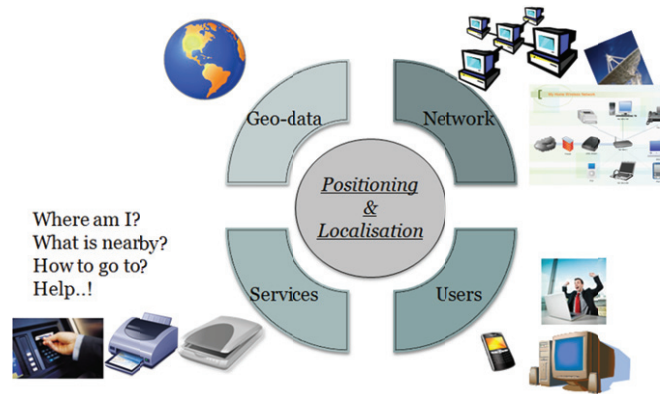

Fig 1. Location based services

   The variety of applications in wireless systems as well as the growing challenges has led to a range of localization techniques developed to meet various constraints [6,7]. Indeed, the approach differs if the system requires physical location (e.g., x-y coordinates or latitude/longitude space) or symbolic (e.g., cell Identity, room number); type of environment (e.g., indoor, outdoor, flat); network topology (e.g., remote sensing, centralized versus decentralized); communication technology and cost (e.g., Bluetooth, infrared, RF); accepted level of uncertainty (e.g., high/moderate/low security level).

   On the other hand, many measurements can be employed for positioning purpose, such as time of arrival (TOA), time difference of arrival (TDOA), angle of arrival (AOA) and received signal strength (RSS) [8]. The latter is usually the cheapest preferred option when one excludes the possibility of adding an extra hardware support to the system in order to ensure, for instance, fine-grain time synchronization required for TDOA and AOA measurements. In this course, one distinguishes the fingerprinting approach [9], which makes use of a training phase where RSS data (fingerprints) are collected from different locations (survey points), yielding a radio map of the deployment area. While in the online stage, the current RSS measurement set is mapped to its best match in the radio map according to the underlying mapping strategy where various machine learning based methods [10] have been put forward for this purpose. But still the problem is very challenging because of the uncertainty pervading the RSS data due to signal fading, signal attenuation as well as the radio propagation model and the non-uniformity of data in radio map (layout of access points is not regular).

   To tackle the above challenge, in continuation of work carried out in [11], this paper presents an RSS based algorithm combining fuzzy methodology with an augmented multi nearest neighbor (kNN) fingerprints, yielding a Multiple Variable Fuzzy Localization (MVFL) algorithm. Especially, a multivariable Takagi-Sugeno (TS) fuzzy inference system [12] was designed to estimate the weight of the target (unknown position) to its (known) neighbors (fingerprints), and use, in turn, such information to estimate its location. Unlike work in [11], different input variables have been employed and a new procedure for identification of parameters of fuzzy system using gradient descent approach together with a set of rational constraints has been introduced. Robust analysis has also been employed to deal with possible outliers and tackle the problem of inappropriate neighbors. The performances of the algorithm have been evaluated using both a simulation platform and real time setting, and compared to some state of art algorithms. The rest of the paper is organized as follow. Section II presents some related work. Section III highlights the main localization algorithms and fingerprinting principle. Section IV deals with radio propagation model employed in this study. Section V presents the proposed MVFL technique. Simulation and experimentation are presented in Section VI and Section VII, respectively.

II.   RELATED WORK

   Since the introduction of IEEE 802.11 standard for implementing WLAN, various methods and technologies have been proposed to address the indoor location estimation problem using the signal strength measurements. The Microsoft Radar system [13] was probably one of the pioneer work in integrating the RSS measurements with a local area map, which, using k-Nearest Neighbor (NN) approach, achieved a localization accuracy of up to 5m. This ultimately assumes that the signal strength of the signal from an IEEE 802.11 access point does not vary significantly at a given location. Several improvements to RADAR's fingerprint matching algorithm have been suggested in [14, 15] for the purpose of improving its accuracy. Support vector machine approach to wireless localization has been advocated in [16] and a comparable performance to kNN approach was reported. Kushki et al. [17] investigated a histogram and Kernel based approach for the same purpose. Wang et al. [18]

investigated the use of WLAN RSS signals for indoor localization in university buildings and labs using empirical models. The original Active Badge System [19] used infrared emitters and detectors to achieve 5-10m accuracy. The Daedalus project [20] developed a system for coarse-grained user location, which coincides with that of the base station to which it is attached to, so that the accuracy is restricted by the radius of the base station. This obviously corresponds to the easiest and simplest fingerprinting like approach. In parallel to WLAN fingerprinting like approach, using short/medium range signals, Laitinen et al. [21] employed GSM-based fingerprinting for outdoor localization where sparse fingerprints from the 6-strongest cells have been collected, achieving 67th percentile accuracy of 44m. Laasonen et al. [22] used the transition between GSM cell towers to build a graph representing the places a user goes to. The Place Lab System [23], whose goal was to provide a coarsegrained accuracy with a minimal mapping effort, uses a map built using a war-driving software and a simple radio model to estimate a cell phone's location with 100-150 meter accuracy in a city environment. On the commercial market, Ekahau [24] has taken a leading role in indoor positioning through a combination of signal strength pattern recognition with an attempt to recover user's history.

Strictly speaking, in order for the aforementioned methods to perform well, a large number of labeled samples need to be collected at each survey point, which is rather context dependent. Indeed, the target environment is critical for the accuracy of WLAN fingerprinting like approach. Beside, radio characteristics in an open environment are never static, and there is no universally fine methodology to tune the data to accommodate environmental change, although, one acknowledges a growing interest in post-deployment adaptation in recent years from telecom industry [25]. Even the commercial products like that provided by Ekahau fall victim to environmental change post-deployment adaptation problems [26]. Consequently, the issue of handling uncertainty pervading the signal strength measurements as well as environmental layout is of paramount importance. This opened the way to alternative uncertainty models like fuzzy logic [27] in wireless indoor location. In this course, one distinguishes two broad classes of solutions. One makes use of fuzzy inference system and the other one advocates a fuzzy clustering related approach, especially fuzzy c-means algorithm (or its variants). The former is based on the idea that the positioning of the (unknown) target node is determined as a weighted combination of (some) fingerprint nodes (or calibrated nodes), where the weights are determined using some fuzzy inference system, see, for instance, [28, 29]. While the latter strategy employs a fuzzy c-means like algorithm to cluster the fingerprint in the RSS space into a certain number of classes. Next, those fingerprints that belong to the same class of the target were selected, and the target position is determined by taking a (weighted) average of the above fingerprints, see, for instance, [7]. Rozyyev et al. [30] combined the idea of fingerprint based on fuzzy inference system with multi-nearest neighbor algorithm to locate objects in wireless sensor networks. The authors showed that fuzzy logic can significantly enhance the accuracy and keep the cost of computation as low as possible. However, given the fuzzy inference system only makes use of one single input consisting of the RSS distance measurements, this renders the approach very limited to handle dynamic environmental changes. This partly motivates our choice to advocate a fuzzy logic like approach for developing our indoor localization algorithm. On the other hand, the choice of fuzzy c-means like approach was discarded mainly because of its computational cost due to its iterative behavior and its sensibility to initialization. In overall this work differs from the aforementioned related works from different perspectives. First, the suggested fuzzy inference makes use of several input variables in order to enhance the robustness of the outcomes (weight parameters). Second, a nonlinear optimization approach based on gradient descent and resilient propagation together with a set of rational constraints that ensure easy interpretability as well as agreement with radio propagation model have been used to estimate the parameters of the fuzzy systems (antecedents and consequents parts of fuzzy "If … then" rules). Third, robust statistical analysis is employed to deal with possible outliers. Fourth, the dynamic change of environment is accounted for through the integration of empirical radio propagation model. Fifth, a comparative analysis will be employed to demonstrate the feasibility of the proposal.

III. FINGERPRINT BASED ON RSS

Location fingerprinting is a location technique that involves a two-stage process: an offline phase and an online phase. In the offline phase, the goal is to build a database for each reference location (fingerprint), say, FP_i by sampling the RSS from several wireless Access Points (APs) yielding vectors *(RSS_{i1}, RSS_{i2},...,RSS_{in})*, i=1 to m, where RSS_{ik} is the signal strength from the ith reference location (fingerprint FP_i(x,y)) to the kth AP, n is the total number of access points and m is the total number of fingerprints [31]. While in the online phase, the location of the target (or target node) *T* with a measured RSS vector is estimated using some pattern matching algorithm by comparing the current observed signal (RSS vector) with pre-recorded values in database. The overall process of fingerprinting localisation system architecture is shown in Fig. 2, where the locations were provided in 2D Cartesian space (although any other reference frame can be used).
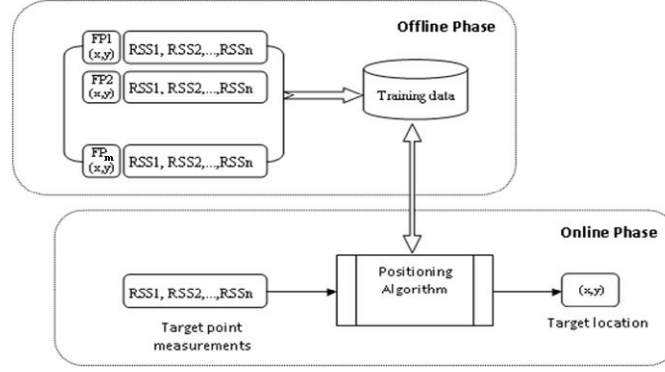
Fig 2 fingerprint block diagram

More formally, given a set of m fingerprints FP_i (i=1 to m) whose data consist of the n-dimensional RSS vectors (RSS_{i1} RSS_{i2} .. RSS_{in}) (i=1 to m), and given an unknown target T whose RSS vector is (RSS_{T1} RSS_{T2} .. RSS_{Tn}), then the similarity between the ith fingerprint and the target can be quantified using the distance:

$$d_{iT} = \sqrt{\sum_{j=1}^{n}(RSS_{ij} - RSS_{Tj})^2} \tag{1}$$

While (1) sounds rational and has been successfully applied in many indoor localization systems including Microsoft Radar project. Nevertheless, in case of missing data from some AP, which often occurs in practice when the signal from one of the APs becomes very weak or not reachable because of some environmental constraint, the qualification (1) becomes inconsistent. An alternative to (1) is rather to take the mean of the distances over the total number of access points reached by both the target and the ith fingerprint:

$$d_{iT} = \sqrt{\frac{1}{n'}\sum_{j=1}^{n'}(RSS_{ij} - RSS_{Tj})^2} \tag{2}$$

Notice that n'$\leq$ n and n'=n in case of full coverage of all APs.

Therefore, several possibilities could be considered for obtaining the location of the target T. This includes:

- Associating the target T with the FP that yields the smallest distance d_{iT} (with respect to i); namely,

$$T(x,y) = AP_k(x,y) \text{ such that } d_{kT} = \min_j d_{jT} \tag{3}$$

This solution corresponds to the proximity like approach in wireless system where the target is collocated with the base station to which it is communicating with [7]. This technique provides symbolic relative location information; when an object is near a known location particularly Radio Frequency Identification (RFID) uses this technique. Another example is the Cell Identification (CID) or Cell of Origin (COO) that are still being used in cellular networks and currently supported by most mobile handsets.

- Use triangulation or lateration to estimate the location of target T(x,y) after converting the RSS distance d_{iT} into Euclidean distance, using some radio propagation model [31]. More specifically, assuming the availability of data from the n access points, this boils down to solving for (x_T, y_T), the following system:

$$\begin{cases} (x_{AP_1} - x_T)^2 + (y_{AP_1} - y_T)^2 = R^2_{1T} \\ (x_{AP_2} - x_T)^2 + (y_{AP_2} - y_T)^2 = R^2_{2T} \\ . \qquad\qquad . \qquad\qquad . \\ (x_{AP_n} - x_T)^2 + (y_{AP_n} - y_T)^2 = R^2_{nT} \end{cases} \tag{4}$$

Where R_{1T} stands for the Euclidean distance from the first access point (AP_1) to target node T, and R_{1T} is usually inferred from RSS map using radio propagation model as will be detailed later on. While (x_{AP_1}, y_{AP_1}) (resp. (x_T, y_T)) stands for the x-y coordinates of the access point AP_1 (resp. T). Nonlinear least square among other techniques can be applied to solve system (4). It should be noticed that the above approach does not make use explicitly of the fingerprint dataset, although some researchers suggested to use such information in the radio propagation when converting the RSS data into Euclidean distance, see, e.g., [6, 33].

- Use of K-Nearest Neighbour (KNN) like approach. In this course, instead of identifying the fingerprint yielding the smallest distance in the RSS space, one relaxes such assumption by considering the K-smallest distance in the RSS space. The position is therefore estimated by averaging over the K closest fingerprints as in (5).

$$x_T = \frac{1}{K}\sum_{i=1}^{K} x_{FP_{\sigma(i)}}, \quad y_T = \frac{1}{K}\sum_{i=1}^{K} y_{FP_{\sigma(i)}} \qquad (5)$$

($x_{FP_{\sigma(i)}}$, $y_{FP_{\sigma(i)}}$) stands for the x-y-coordinate of one of the fingerprints among those in the K-nearest neighbors; namely, σ corresponds to a permutation of the indices of m fingerprints such that σ(1) corresponds to the index of the nearest neighbor, σ(2) is the second-nearest neighbor, and so on. Similar approach has been implemented in Microsoft Radar project [13]. This is motivated by the inherent variability of the signal strength, making the restriction to the nearest fingerprint is not a rational option. On the other hand, it has been suggested [13] that the error vector (in physical space) corresponding to each neighbor is oriented in a different direction. Therefore, averaging the coordinates of the neighbors may enhance the accuracy of the positioning of the target. Instead of standard arithmetic average, weighted average approach can also be used, where the weights depend on some external factors (e.g., distance to access points) [33]:

$$x_T = \frac{1}{K}\sum_{i=1}^{K} w_i x_{FP_{\sigma(i)}}, \quad y_T = \frac{1}{K}\sum_{i=1}^{K} w_i y_{FP_{\sigma(i)}} \qquad (6)$$

The weights w_i are such that $\sum_{i=1}^{K} w_i = 1$

A simple configuration of the weights yielding a weighted K-NN consists in choosing the weights proportional to the target-neighbor distance.
- Machine learning related approaches [10], including neural network, support vector machine, support vector regressions, histogram and kernel methods as well as fuzzy approaches [28-30] have also been suggested to handle the positioning aspect. Strictly speaking, most of such techniques rely on the generalization power of the underlying method where the offline phase was used as a reference point from which new measurement is compared with. For instance, the fingerprints collected during the offline stage are used to train the neural network and obtain optimal weights, then estimate the location based on determining the output from the neural network with the weights matrix generated at earlier stage [6,7, 34]. Consequently such approaches can be employed in conjunction or as extension to (5-6) expressions.

Nevertheless, it should be noted that, despite their popularity and the growing range of products employing such approach, fingerprinting for indoor WLAN environment performance still is limited by some growing challenges. First, most of the indoor WLAN are implemented using the 2.4 GHz public band WLAN frequency proposed by IEEE 802.11 which is also used by GSM, microwave and other wireless devices. This may cause irregular RSS patterns to the collected data in offline stage (fingerprints collecting stage). Second, the availability of blocking bodies in the indoor environment could weak the signal and could hide the LOS between AP and receivers. Third, the accuracy of fingerprinting methods heavily relies on the density of fingerprints collected during the offline phase, where, on long term run, any change in the environment such as Access Point (AP) replacement, facilities upgrade, etc, can lead to poor system performance. Indeed, if for any reason one of the reference nodes vanished from the map, the algorithm will end selecting a point with larger Euclidean distance, and this will negatively impact the accuracy of estimation. This motivates the need to account for physical signal properties when using the RSS data. More specifically, the use of appropriate radio propagation model that accounts for such irregularities contributes significantly to the performance of the underlying fingerprinting application. Our approach for such issue is detailed in next section.

IV.   RADIO PROPAGATION MODEL

Radio propagation model [1] describes the signal attenuation with respect to the distance between emitter (access point) and receiver. Strictly speaking, the signal strength always decreases with the distance, however, several parameters have non-negligible influence on such attenuation. This includes multipath effects due to reflection, refraction and scattering, fading, absorption due to physical properties of materials, and random noise. These variations can be classified into three main classes [15]:

- *Temporal variations:* when the user stands at fixed position, the signal strength measured varies over time due to the physical environments such as people movement.
- *Large-scale variations:* the signal strength varies over long distance due to attenuation, leading to change in the signature of the fingerprints.
- *Small-scale variations:* this happens when the user moves over a small distance (order of wave length), which affects the average received signal strength.

Temporal variations are usually dealt by storing the entire histogram of RSS acquired during the offline phase in the radio map instead of average RSS values only, and possibly with storing second order statistics or so. While small-scale variation are tackled through by deleting the effect of the variation then compensate it in the location estimation [15], although the appropriate identification of such compensation is still an open issue especially in dynamic environment. Large scale variations are typically handled by radio propagation model whose attenuation strictly increases with the distance.

Consequently, building a generic propagation model is very difficult and not an option. Our interest focuses on the radio propagation model put forward in [35], which has been tested in indoor environment close to that experienced in this paper. The model describes the path loss value PL, which expresses the difference between the received signal strength and the transmitted signal strength, as a function of the distance d (in meters) between the transmitter and receiver.

$$PL_{dB-2.4\,indoor} = -40 - 31log_{10}(d) \pm 8 \qquad (7)$$

Interestingly, the model in (7) includes an uncertainty element constituted of ± 8, which describes an upper and lower bounds to the path loss. This would be especially interesting when eliciting the fuzzy membership functions as will be explained in the next section.

Strictly speaking, model (7), also joins alternatives indoor propagation models, like that put forward in [34]
$$PL_{dB-2.4\,indoor} = R_0 - 10\alpha log_{10}(d) - \beta \qquad (8)$$

With R_0, α and β taking different values depending whether the situation is LOS or NLOS. Given the uncertainty to determine beforehand the situation that will occur in a dynamically changing environment, (7) seems to be a rational choice that accounts for such doubt. A simulation of model (6) is shown in Fig. 3.
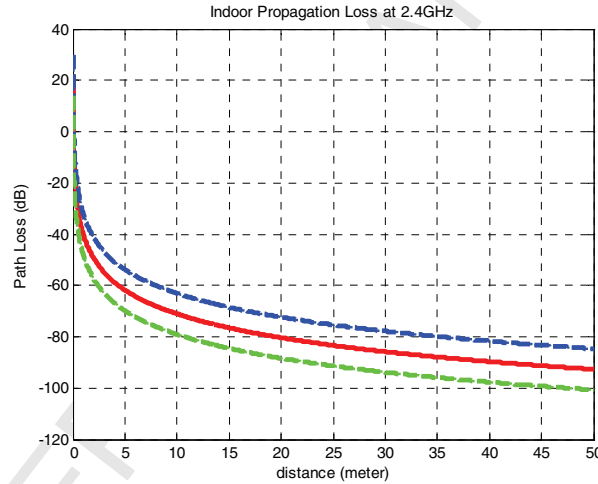
Fig. 3. Radio Propagation model

The results of the plot, which were also confirmed through authors' experiments conducted at local offices with inner walls made of gypsum boards, show about 70dB of power lost in the first meter and a maximum distance that a 2.4GHz system with range of 80dB and zero gain antennas can achieve is about 20 meters.

The idea of modelling indoor path loss propagation was utilized in the localisation process by many researchers. For example in [36], ANFIS system was used to model the propagation of signal with the environment based on collected RSS at certain locations (fingerprints) and then the model was verified with curve fitting technique before being used in the localization process, although this model showed better performance than the one with curve fitting technique only, but it was not evaluated against accidental environment changes.

V. MULTIVARIABLE FUZZY LOCALIZATION (MVFL)

A. *Overall Architecture*

Similarly to work carried out in [30], a fuzzy inference system is applied to find out weights attached to the K-nearest neighbor fingerprints. Then, the location of the target node is determined as the weighted combination of these K-nearest neighbor fingerprints in the light of expression (6).

Therefore, the first phase consists in determining the K-nearest neighbors. This is performed by calculating the distances in RSS space from each fingerprint to the target in the sense of expression (2), and then selecting the fingerprints yielding the K smallest distances.

Now in order to determine the weights in (6), a fuzzy inference system has been put forward. The proposal makes use of two input variables:
- The distance D(j) (j= 1 to K) in RSS space from the target node to the jth nearest neighbour fingerprint.
- The difference of the signal variations V_j between target node and j^{th} nearest neighbour with respect to different APs.

The output of the fuzzy system consists of the weight attached to each fingerprint belonging to the set of K-nearest neighbor. We adopted Takagi-Sugeno (TS) fuzzy system as the main fuzzy inference system. The main feature of T-S fuzzy models is that they characterize the local dynamics of each fuzzy rule by a linear model. In our system, as it will be detailed later on, the outcome is constant. The generic system is shown in Figure 4.
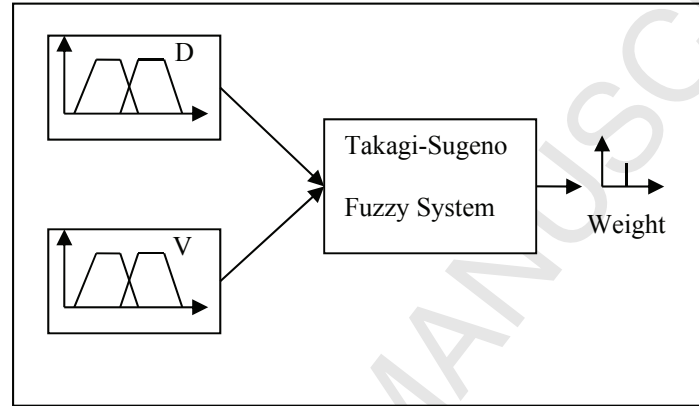
Figure 4. General block diagram

More formally, the input variables are expressed as

$$D(j)= \sqrt{\frac{1}{n}\sum_{i=1}^{n}(RSS_{ji} - RSS_{Ti})^2}, \tag{9}$$

$$V(j) = \left| \left(\max_i RSS_{ji} - \min_i RSS_{ji} \right) - \left(\max_i RSS_{Ti} - \min_i RSS_{Ti} \right) \right| \tag{10}$$

$$j \in \{\sigma(1), \sigma(2), \dots, \sigma(K)\}$$

Strictly speaking, the input variable $V(j)$ allows us to control the extent to which both the target and the underlying fingerprint agree in terms of the total variations caused by the use of distinct access points. Indeed, it is trivial that the distance is not a sufficient indicator to discriminate between distinct scenarios. For instance, geometrically speaking, points located on the same circle have equal distance to the center of this circle even if they may be very disparate from each other. Consequently, adding an extra discrimination parameter sounds intuitively useful. In the same spirit, authors in [29] have employed standard deviation statistics as an extra discriminating variable.

Therefore, the more a given fingerprint agrees with the target node in terms of both distance D and variation V, the more important is the weight associated to the underlying fingerprint. In order to quantify this statement in fuzzy logic, a set of "if.. then.." (fuzzy) rules are elaborated. For instance,
- IF D(j) is *Very Small* AND V(j) is *Very Small* THEN weight of jth fingerprint is *Very High*
- IF D(j) is *High* AND V(j) is *High* THEN weight of jth fingerprint is *Very Low*.
- IF D(j) is *High* AND V(j) is *Small* THEN weight of jth fingerprint is *Very Low*.

The above linguistic qualifications are obtained through fuzzification process where the (crisp) inputs are transformed into fuzzy sets. The latter are characterized by their membership functions, which describe the shapes. Typically, simple parameterized models, e.g, Gaussian, triangular, trapezoidal, S-shape, were used in the literature. In our model, trapezoid membership functions were employed in our system.

Fig. 5. Fuzzification of Input Variable D (or V)
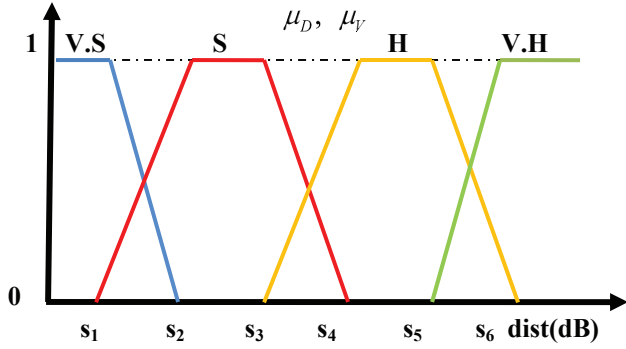
According to Fig. 5, the assignment of a specific (fuzzy) linguistic quantifier to the distance d (in signal space) output depends on its numerical value. More formally, we have for instance
- If $d \leq s_2$, then d (in dB) is classified as Very Small (VS)
- If $s_1 \leq d \leq s_4$, then d is classified as Small (S)
- If $s_3 \leq d \leq s_6$, then d is classified as High (H)
- If $d \geq s_5$, then d is classified as Very High (VH)

On the other hand, the determination of the boundary of the membership functions in Fig. 5 obeys some rational criteria. This includes:
  i)   easy interpretability;
  ii)   respect of physical and statistical characteristics of the RSS;
  iii)   agreement with one of membership function interpretations;
  iv)   existence of sufficient number of (fuzzy) rules could be activated;
  v)   minimization of predicted output and ground truth.

Especially, requirements (ii) also imposed some constraints on the simulation and experiment setup later on. Indeed, given that the RSS values fail sharply in the first meter or so (around 70dB) as opposed to smooth transition in the range 1m-50m, therefore, we deliberately chosen situations in which the APs and fingerprints / target were at least one meter distant in order to ensure smooth coverage of the whole RSS range. More detailed handling of the above constraints are highlighted in next section.

B. *Fuzzy System Parameter Identification*

First in order to ease the comparison with previous work, we consider the output of the fuzzy system to be a numerical constant value, this makes the underlying fuzzy system coincides with zero-order Takagi-Sugeno fuzzy system [12]. The ith rule can be formulized as:

R^i: IF D is F_D^i AND V is F_V^i THEN W is θ_{VD}^i

Where F_D^i and F_V^i are fuzzy sets associated to variables D and V, respectively, while θ_{VD}^i stands for a constant value associated to weight W, for the rule R^i. In accordance to fuzzy operators where the fuzzy connective AND is implemented using the product operator, then assuming the center of area like defuzzification, the output associated to M fuzzy rules is provided by [27]:

$$\hat{w}(V,D) = \frac{\sum_{i=1}^{M} \theta_{VD}^i \mu_{F_V^i}(V) . \mu_{F_D^i}(D)}{\sum_{i=1}^{M} \mu_{F_V^i}(V) . \mu_{F_D^i}(D)} \tag{11}$$

Where the membership functions $\mu_{F_V^i}$ and $\mu_{F_D^i}$ are defined as trapezoidal function as pointed out previously in Section A through their associated four parameters defining the support and core of the membership function, so that

$$\mu_{F_V^i}(V) = \begin{cases} 0 & \text{if } V < v_1^i \text{ or } V > v_4^i \\ \dfrac{V - v_1^i}{v_2^i - v_1^i} & \text{if } v_1^i \le V \le v_2^i \\ 1 & \text{if } v_2^i \le V \le v_3^i \\ \dfrac{v_4^i - V}{v_4^i - v_3^i} & \text{if } v_4^i \le V \le v_3^i \end{cases} \quad \text{and} \quad \mu_{F_D^i}(D) = \begin{cases} 0 & \text{if } D < \rho_1^i \text{ or } D > \rho_4^i \\ \dfrac{D - \rho_1^i}{\rho_2^i - \rho_1^i} & \text{if } \rho_1^i \le D \le \rho_2^i \\ 1 & \text{if } \rho_2^i \le D \le \rho_3^i \\ \dfrac{\rho_4^i - D}{\rho_4^i - \rho_3^i} & \text{if } \rho_4^i \le D \le \rho_3^i \end{cases} \qquad (12)$$

The problem of fuzzy system identification boils down to estimating the parameters of the fuzzy systems; namely, v^i and ρ^i, which correspond to antecedents parts of rule R^i and the consequent part θ_{VD}^i. From a set of observation (V_i, D_i, w_i) i=1,N, the estimation of the parameter vector should also minimizes the estimation error

$$J(v, \rho, \theta) = \sum_{i=1}^{m} \left[\left(w_i - \hat{w}(v_i, \rho^i, \theta_{VD}^i) \right) \right]^2 \qquad (13)$$

Notice that the weights w_i issued from the observation are quantified according to the distance of the underlying fingerprint to the known target so that the more the location of the fingerprint is close to the (true) target, the higher is the associated weight. More formally, given a target T in x-y coordinates and a fingerprint P_i yielding (V_i, D_i) measurement, then weight is given as

$$w_i = \begin{cases} 1 & \text{if } \text{dist}(P_i, T) < \tau_1 \\ 1 - \dfrac{\text{dist}(P_i, T)}{\tau_2} & \text{if } \tau_1 \le \text{dist}(P_i, T) \le \tau_2 \\ 0 & \text{if } \text{dist}(P_i, T) > \tau_2 \end{cases} \qquad (14)$$

Where *dist* stands for distance in Euclidean space, and τ_1 and τ_2 are thresholds on distance delimiting the full coincidence with target node and full separation, respectively.

Strictly speaking, one may distinguish at least two streams of research in the estimation of the fuzzy system parameters. The first one advocates the use of a two stage strategy where the antecedent parts v^i and ρ^i (i=1 to M) of the membership functions were identified through clustering [39-41] or neural network / genetic algorithm like approach [42-47]. Next, the consequent parts were determined, usually using least square algorithm [12]. The second stream involves the use of optimization like approach such as gradient descent where all parameters are learned through iterating with constant adjustment factor until a satisfactory level of performance metric, usually estimation error, is reached [48-50]. Hybrid approaches employing both gradient descent and clustering and/or least squares can also be envisioned. Besides, the number of partition of the input space v and D, which controls the number of total fuzzy rules M, can also be used as part of system identification. For this purpose, usually inter-class validity criteria is used in case of clustering based approach, while it can also be part of parameters to be identified in case of gradient descent like approach. On the other hand, it is also worth pointing that both clustering and gradient descent like approaches may lead to non-appealing result where there is less or full absence between fuzzy sets, which, in turn, result in weakly activated or not activated at all fuzzy rule (s) for some combination of input space, see for instance [51] and references therein. This yields into relaxation of optimality criteria governing either the clustering or the gradient descent like approaches. Even early work of Sugeno and Yasukawa [52] fit into this category. This motivates our approach to employ the gradient descent approach in order to estimate both the antecedent and the consequent parts of the rule in conjunction with a set of rational constraints that ensure full comply with desirable requirements set in Section A. Especially, in order to ensure requirement (i) and (iv), we consider that, for a given input variable, for any fuzzy set, there is always one fuzzy for which the overlapping part has a membership grade of 0.5 as it can be seen in the example of Fig. 5. Besides, in order to ensure requirement (ii) and (iii), the range of the values that can be assigned to the input variable is determined by the physical and statistical characteristics of RSS. The latter are simulated using the simulated environment as well as the radio propagation model (7) as will be detailed in Simulation section of this paper. In this context, the core and support of the membership function can be interpreted as the extent of the interval where the true boundary of the distance in signal space will possibly and certainly lie in, respectively. This agrees with the random set view interpretation, where the membership function is viewed as a nested family of level-cuts [36].
More formally, the determination of the fuzzy system parameters boils down to the following optimization problem:

$$\underset{\theta, \mathbf{v}, \rho}{Minimize} \quad J(\mathbf{v}, \rho, \theta) = \sum_{i=1}^{m} \left[(w_i - \hat{w}(v_i, \rho^i, \theta_{VD}^i)) \right]^2 \tag{15}$$

such that

$$\forall V_i \in U_V, \ \sum_{i=1}^{M_1} \mu_{F_V^i}(V_i) = 1, \ i=1,m \tag{16}$$

$$\forall D_i \in U_D, \ \sum_{i=1}^{M_2} \mu_{F_D^i}(D_i) = 1, \ i=1,m \tag{17}$$

$$[\inf(v) \ \sup(v)] = f(RSS) \tag{18}$$
$$[\inf(D) \ \sup(D)] = g(RSS) \tag{19}$$

Expression (15) is in agreement with requirement (v) where the estimated parameters constituted of rule premise antecedents part **v** and ρ as well as consequent parts θ are the unknown variables.

Expressions (16) and (17) state that for each value of the input variable V and D belonging to the corresponding universe of discourse U_D and U_V, then the sum of membership grades associated to all fuzzy sets of the partition (M_1 partition for input variable V and M_2 partition for variable D) is equal to unity. This insures for instance that for each value of the input variable, there is at least one rule which is activated. If there is an overlapping between two fuzzy sets, then the maximum membership grade of the overlapping area is equal 0.5. This guarantees the interpretability requirement stated earlier. Finally, expressions (18-19) indicate that the range of values associated to universe of discourse of the two input variables is function of the signal strength values.

In order to implement the above optimization problem a gradient descent method is applied, similar to work in [49,50]. Besides, in order to strengthen its computational complexity, we used resilient propagation RPROP [53], initially developed for neural network training, and employs a gradient descent algorithm with a resilient parameter update step. A link of RPROP with Matlab FIS system environment is also established in order to ease the solution of the above constrained optimization problem. Besides, the fact that the trapezoidal functions are piecewise derivable makes the use of the RPROP appropriate. On the other hand, the number of partition is taken constant $M_1=M_2=4$, yielding a total of M=4 x 4 = 16 rules. This is mainly motivated on one hand, by the desire of simplification of the above optimization problem, and the ease of comparison with alternative approaches on the other hand.

Strictly speaking, an alternative implementation would be to work out the augmented Lagrangian operator from (15-17) as

$$\underset{\theta, \mathbf{v}, \rho, \lambda, \chi}{Minimize} \quad J(\mathbf{v}, \rho, \theta, \lambda, \chi) = \sum_{i=1}^{m} \left[(w_i - \frac{\sum_{j=1}^{M} \theta_{VD}^j \mu_{F_V^j}(V_i).\mu_{F_D^i}(D_i)}{\sum_{j=1}^{M} \mu_{F_V^j}(V_i).\mu_{F_D^j}(D_i)} \hat{w}(v_i, \rho^i, \theta_{VD}^i)) \right]^2 + \sum_{i=1}^{m} \lambda_i \sum_{j=1}^{M_1} (1 - \mu_{F_V^j}(V_i)) + \sum_{i=1}^{m} \chi_i \sum_{j=1}^{M_1} (1 - \mu_{F_D^j}(D_i)) \tag{20}$$

And then set the derivatives with respect to antecedent, consequent rule parameters as well as Lagrange multipliers λ, χ to zero, yielding a solution close to clustering like fuzzy identification approach. Nevertheless such solution has not been pursued due to already proven efficiency of RPROP and less sensitivity to initial guess, besides, alternative studies have shown that even applying much more exhaustive search strategies i.e., Johansen and Foss [54] only marginally outperform RPROP.

Complexity

The complexity of one single iteration of RPOP algorithm with an input of size N and M number of rules with L patterns yields a linear complexity of O(NML), and given that the total number of iterations is set to an upper bound even if the convergence criteria is not met, so the overall complexity can be linearly approximated.

Using a standard PC configuration of Intel Celeron Dual Core 1.8 GHz and 8GB of RAM, a single iteration is executed in a fraction of second only (around 0.06s).

The nonlinear optimization involving EPROP is initialized similarly to configuration of Fig. 5 but where the membership functions form almost equal symmetrical partition. The solution of this optimization problem yields, after rounding up to their closest integer values, the distance in RSS space of s_1, s_2, s_3, s_4, s_5 and s_6 as 2, 5, 9, 14, 17 and 22dB, respectively, for input variable D. Similarly, for input variable V, the obtained values for s_1, s_2, s_3, s_4, s_5 and s_6 of Fig 5 are 3, 7, 10, 13, 19 and 26dB, respectively. Intuitively, values of variables V induce wider variations of RSS distance values than that of variable D whose range is rather close to average evaluations as it can be seen from expressions (9) and (10). The final configuration of the partition is closed to that provided in Figure 5. The obtained antecedent parts constituted of the weights θ_{VD}^i associated to each rule of the sixteen rules are provided in Table 1.

Table 1. Fuzzy Rules

D / V	VS	S	H	VH
V.S	1	0.83	0.54	0.03
S	0.95	0.56	0.16	0.05
H	0.86	0.47	0.01	0
VH	0.81	0.42	0	0

For example, some rules read as
- If D is Very Small and V is Very Small then Weight is equal to 1.
- If D is Very Small and V is Small then Weight is equal to 0.95.
- If D is Small and V is Very Small then Weight is equal to 0.82.
- If D is High and V is Very High then Weight is zero.
- Etc.

The total number of Takagi-Sugeno fuzzy rules is 4 x 4 = 16 rules, since there are four fuzzy sets for each input (V and D). In some situations, and given the overlapping among fuzzy variables in Fig. 5, it may happen that several rules are activated to reflect the fact that for some cases, there is no single answer at a specific input value. Nevertheless, there is no situation in which there is no rule activated for a particular set of input variables, which shows that requirements (i) and (iv) are met.

Now in order to highlight the functioning of the T-S Fuzzy inference system, and its link to the target positioning estimation, one shall first detail the basis fuzzy inference system. The latter as discussed in [27] can be broken down into four parts: 1) mapping each of the crisp inputs into a fuzzy variable (fuzzification); 2) determining the output of each rule given its fuzzy antecedents; 3) determining the aggregate output(s) of all of the fuzzy rules; 4) mapping the fuzzy output(s) to crisp output(s) (defuzzification). More specifically, given, for example, two realizations of input variables D and V, two possible rules can be enabled as:

If D is A_1 and V is B_1 Then W is C_1.

If D is A_2 and V is B_2 Then W is C_2.

Where A_1, B_1, A_2, B_2 stand for any of VS, S, H, VH fuzzy sets and C_1, C_2 stand for any values in set {1, 0.95, 0.86. 0.83, 0.81, 0.56, 0.54, 0.47, 0.42, 0.16, 0.05, 0.03, 0.01, 0}.

The two crisp values d and v of the two antecedents (or inputs) D and V are fuzzified by two fuzzy singletons. Based on the intersections of antecedent (or premise) membership functions with input singletons, the rule firing strengths are computed as:

$$\mu_{firinng,1} = h_1 = \mu_{A_1}(d) \wedge \mu_{B_1}(v)$$
$$\mu_{firinng,2} = h_2 = \mu_{A_2}(d) \wedge \mu_{B_2}(v)$$

(21)

Where the AND operator $\wedge$ is rather implemented using arithmetic operation in the same spirit as (11), but usually any other t-norm like operator [27] can also be employed. The rule firing strength is also called *premise membership grade* or the rule *validity index* at the given crisp inputs.

Denoting by E_1 and E_2, the outcomes of the first and second rule (in terms of value of weight W) for specific realization d and v of D and V, then the overall outcome of both rules will be

$$E = \frac{E_1 h_1 + E_2 h_2}{h_1 + h_2}$$

(22)

Defuzzification allows us to extract a single (crisp) value from a fuzzy set. Typically, there are several defuzzification methods available in fuzzy logic literature for computing the crisp output of a fuzzy system. Two of the popular methods are discussed here. These are Centre of Area (COA) method and Centre-average (CA) method. In case of Takagi-Sugeno System, the defuzzification is carried out by the weighted average expression as in (22). A graphical illustration of the above processing is highlighted in Fig. 6.
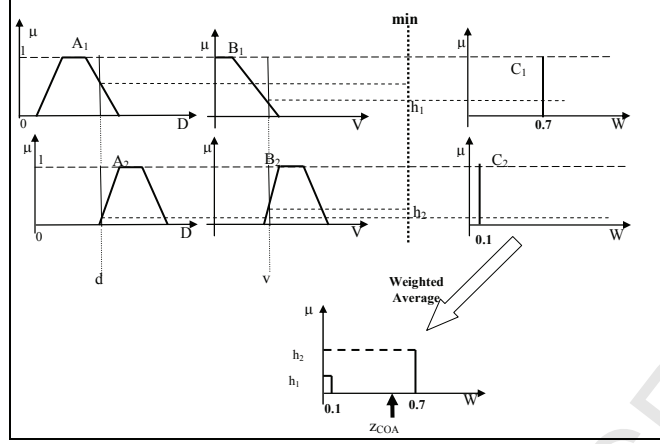
Figure 6. Illustration of T-S Inference system

Now the estimation of the target coordinates is therefore driven from the coordinates of the fingerprints (in the set of K-nearest neighbours) and the associated weights outputted by the fuzzy inference system using a weighted average, so that:

$$
x_T = \begin{cases} \dfrac{\sum\limits_{i=1}^{K} w_i x_{FP_{\sigma(i)}}}{\sum\limits_{i=1}^{K} w_i} & \text{if } \sum\limits_{i=1}^{K} w_i \neq 0 \\[2em] \dfrac{1}{K} \sum\limits_{i=1}^{K} x_{FP_{\sigma(i)}}, & \text{otherwise} \end{cases}
\tag{23}
$$

$$
y_T = \begin{cases} \dfrac{\sum\limits_{i=1}^{K} w_i y_{FP_{\sigma(i)}}}{\sum\limits_{i=1}^{K} w_i} & \text{if } \sum\limits_{i=1}^{K} w_i \neq 0 \\[2em] \dfrac{1}{K} \sum\limits_{i=1}^{K} y_{FP_{\sigma(i)}}, & \text{otherwise} \end{cases}
\tag{24}
$$

Note that (23-24) is induced from expression (6) when the weights were not normalized. The symbols in (23-24) were defined similarly as in (6).

C. *Some properties of MVFL*

Based on the values of input variables V and D, some useful cases regarding the performance of the MVFL algorithm can be distinguished.

Proposition 1
If the fingerprints outputted by the KNN are such that
  $\max(D_i, V_i) \leq s_1$ for some nearest neighbor i, and
  $\min(D_j, V_j) \geq s_6, \quad \forall j=1,K, j \neq i$

Then, the outcome of MVFL coincides with the ith nearest fingerprint.

Proof

The proof of the above proposition follows straightforwardly from the fact that the condition $\max(D_i, V_i) \leq s_1$ entails that both D_i and V_i are evaluated Very Small and there is only one single fuzzy rule activated. This yields according to Table 1 a maximum weight of 1 attached to i^{th} nearest neighbor, while the statement $\min(D_j, V_j) \geq s_6, \quad \forall j=1, K, j \neq i$ ensures that all other nearest neighbors were evaluated to High for both input variables D and V, which again, according to Table 1 and uniqueness of fuzzy rule activated, yields a zero weight attached to those fingerprints. Therefore applying (14-15) yields straightforwardly result pointed out in Proposition 1.

Proposition 2
If the fingerprints outputted by the KNN are such that
$$\min(D_j, V_j) \geq s_6, \quad \forall j=1, K$$

Then, the outcome of MVFL almost coincides with that of the standard KNN using (5).

The proof of Proposition 2 follows the same spirit as that of Proposition 1. That is, the condition stated in the body of the proposition entails that all nearest neighbors were evaluated to High for both V and D inputs, which, together with uniqueness of activated fuzzy rule (s), yields almost a zero-valued weight (0.01) attached to each nearest neighbor. Therefore the application of (22-23) yields the same result as (5)

Proposition 3
If the fingerprints outputted by the KNN are such that
$\max(D_i, V_i) \leq s_1$ for all nearest neighbor i (i=1, K), then, the outcome of MVFL coincides with that of standard KNN using (5)

Again this follows from the fact that the condition in Proposition 3 entails that all nearest neighbors were evaluated to Vey Small for both input variables, yielding maximum weight value 1. The detail proof is omitted for its simplicity.

Notice that, interestingly, MVFL induces the same result as standard KNN when either both input variables were evaluated Very Small or High. Trivially, the above result still is held when both input variables were evaluated Very High.

VI. SIMULATION

To evaluate the proposal a testbed was constructed using 4 APs mounted in the corners of 20x20 meters area with coordinates AP1(0,0) AP2(20,0) AP3(20,20) and AP4(0,20). 64 fingerprints were specified in symmetric way with approximately 2.2 meter space, and 16 random testing targets to be localised were generated with known coordinates, as shown in Fig 7. The simulation setup was chosen for its similarity with experiment layout that will be described later on.

The radio propagation model pointed out in expression (7) was used to construct the RSS map for the fingerprints and targets. In the offline phase the radio map is created by calculating the physical distance from every fingerprint to each AP, using the initial (known) x-y coordinates. Then, the propagation model (7) is used to generate fingerprint's RSS values. More formally, its implementation induces the calculus for every (true) distance from the given j^{th} fingerprint to a given i^{th} AP, the expression

$$RSS_{ij} = -40 - 31\log_{10}(d_{ij}) + \varepsilon \quad , \tag{25}$$

where d_{ij} stands for the distance from the jth fingerprint to the ith access point. While ε stands for the Gaussian random noise of zero mean and standard deviation 2dB. The latter was introduced to account for a bounded uncertainty of 8dB in (7). Indeed, using the fact that, for a zero-mean Gaussian signal of standard deviation σ, the range of the underlying random variable is approximately bounded by [-3σ 3σ], therefore, to account for a bounded uncertainty of 8dB, a random Gaussian zero mean and standard deviation 2dB sounds rational.

For each fingerprint j, one therefore generates a vector of RSS values where each component corresponds to the associated signal strength from a given AP to the jth fingerprint. The dimension of such vector is equal to the total number of access points. The set of all such vectors pertaining to all fingerprints constitutes the offline stage of the fingerprinting localization approach. It should be noted that in case where all APs were visible to all fingerprints, the dataset of the offline phase boils down to standard m x n matrix (where m and n stand for the number of fingerprints and AP, respectively).
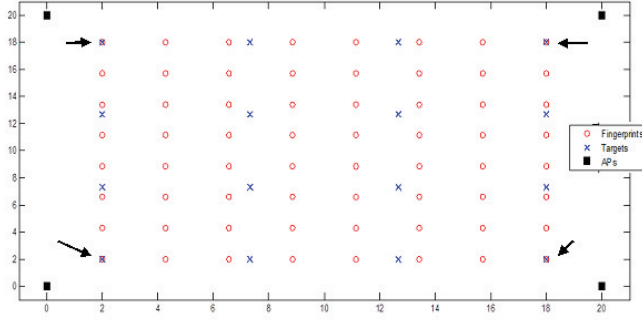
Fig 7 MVFL Testbed

In the online phase, the K-nearest neighbour (kNN) algorithm is first used to identify the K closest neighbours for a given target according to the Euclidean distance in equation (2). Then the distances D and V (in signal space) for each closest neighbour, will be used as inputs to the multivariable Takagi-Sugeno fuzzy inference system, which, in turn, determines the weight associated to each fingerprint of the K-nearest neighbour. Finally, the positioning of each target is estimated using (22-23). A pseudo-code of the overall methodology is summarized in Figure 8.

```
OFFLINE STAGE
 FOR Each Access Point i
 FOR Each Fingerprint j
   Compute Euclidean distance d(i,j)
   Compute RSS(i,j) using (24)
   Store RSS(i,j)
 END
 END

ONLINE STAGE
For each target T
  Calculate K-nearest neighbours fingerprints to T
  FOR each nearest fingerprint i (i=1 to K)
   Calculate ViT  using (10)
   Calculate DiT using (9)
   Input ViT and DiT to T-S fuzzy inference system
   Collect the weight wi of fingerprint i
 END
  Estimate the location of target T using (23-24)
 AND
```

Figure 8. Overview of offline/Online stage of simulation setup

Given the knowledge of the true position of the target from the user's perspective, the performance of the developed fuzzy positioning system can be evaluation using standard root mean square error (RMSE) metric; namely:

$$Error = \sqrt{(X_{\mathrm{T}} - X_{TAct})^2 + (Y_{\mathrm{T}} - Y_{TAct})^2}$$

(26)

Where X_{TAct}, and Y_{TAct} are the actual coordinates of target T. The results of this technique are compared to K-NN combined with single variable fuzzy localization (SVFL)[1] proposed in [30], as well as the standard K-NN, weighted K-NN and triangulation approach (See appendix for details calculus of triangulation approach). First, in Fig. 9 is shown the positioning of the target within the environmental layout. It is also shown the true (actual) position of the targets as well as their estimations using alternative (average) KNN approach. A total of sixteen test points (target nodes) randomly generated in the environment layout, were employed. The graph illustrates the good performance of the developed MVFL algorithm as demonstrated by the closeness of the estimated target position to the actual (true) position. Besides given the randomness inherent in parameter ε of expression (15), the calculus of the estimation is averaged over 100 Monte Carlo simulations. This process is repeated for both

---

[1] It should be noted that the implementation of SVFL here is adapted to accommodate the input fuzzification employed in this paper with fuzzy rules like "if D is very small then Weight is one", "If D is small then Weight is 0.5", "If D is high then Weight is 0.25", "If D is very high then Weight is 0".

offline and online phases. Although, for the offline stage, the process is only performed once in order to build the radio map. The dataset issued from the radio map are then called upon by each fingerprinting algorithm to calculate the position of the target. Fig. 10 illustrates the performance of the MVFL algorithm with respect to root mean square error metric for each target. Namely, the x-coordinate in Fig. 10 corresponds to the target label (first target, second target, etc.) and not the number of targets as it may sound like.
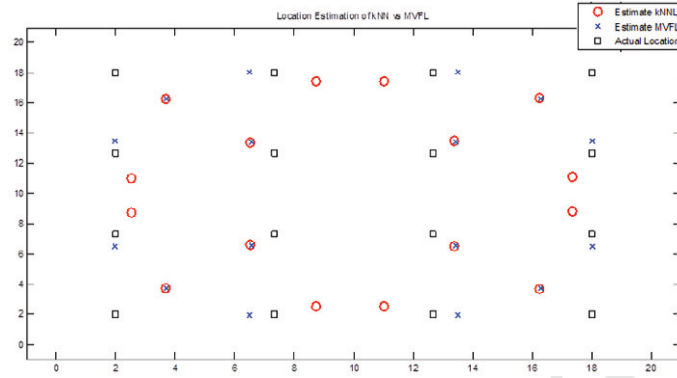

Fig. 9. Actual location ( ) vs. estimated location of kNN (o) and MVFL (x)

The plot also displays the performance of alternative positioning algorithms (average KNN, Weighted KNN, SVFL and triangulation or lateration -LAT).
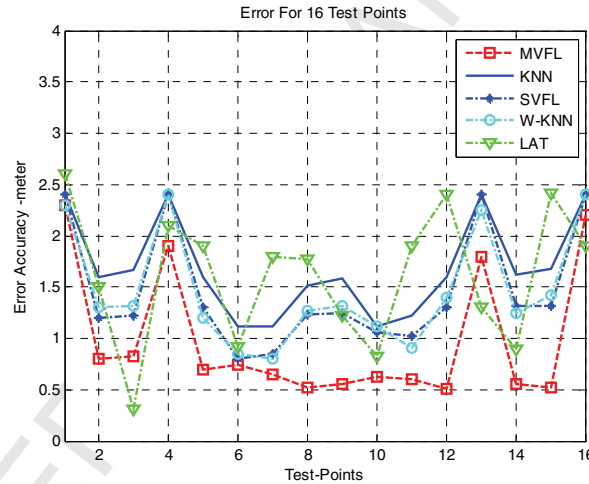

Fig 10. Error in estimation of kNN vs MVFL

It is worth pointing out from figures 9 and 10 that the MVFT outperforms the K-NN localization algorithm, as well as other alternative approaches discussed later on. However, in case where the target node coincides with a given fingerprint as those symbolized by an arrow in testbed of Figure 7, one notices that MVFT evaluation degrades slightly to almost coincide sometimes with that of K-NN in Fig.10. This can be explained through several arguments. First, the fact that target is generated at same location as a given fingerprint does not mean necessarily that the associated RSS value also coincides with that of fingerprint due to effect of randomness. Otherwise, if conditions of Proposition 1 were met, the algorithm would provide as stated in Proposition 1 a fully accurate result consisting of the position of the underlying fingerprint. Second, given the nature of RSS space and the fuzzification of the distance parameter D and V, it is not fully excluded that both input variables will be evaluated to very small, yielding according to Proposition 3 a result which coincides KNN result. Third, the number of nearest neighbours K plays also a non-negligible role. Indeed, for our case, with K=3, which was found to perform well, the algorithm (both K-NN and MVFT) tends in such situation to locate the target within a triangle constituted of the three nearest neighbours. Roughly speaking to handle such scenario, a trivial solution consists to reduce substantially the value of K to a singleton. However, although, such solution seems to be appropriate for this special case, provided that signal strength of the target were very close to that of the underlying fingerprint, it will cope poorly with the vast majority of cases in which the testdata do not coincide with any fingerprint.

Next, in order to compare more efficiently the performance of the developed algorithm, one considers situations of various noise intensities, and one evaluates the RMSE value of each positioning algorithm. For this purpose, the RSS value corresponding to the target (node) is modified to account for the noise intensity. This boils down to rewriting expression (24) as

$$RSS_{iT} = -40 - 31log_{10}(d_{iT}) + \varepsilon_\sigma \quad , \tag{27}$$

where ε_σ is now zero-mean Gaussian noise with (variable) standard deviation σ. Notice that (25) is only applied to the generated RSS value of the target T to each access point, while the RSS values of fingerprints remain unchanged with respect to that already stored in the radio map. The result provided in Table 2 corresponds to the average across all testdata (the sixteen targets) of the RMSE quantification.

Table 2. MVFL vs. kNN with different noise intensity

Noise level SdB	Average Accuracy Error				
	kNN	MVFL	SVFL	W-KNN	LAT
1	1.32	0.61	0.88	0.86	0.51
2	1.69	0.82	1.41	1.47	1.60
3	1.94	0.81	1.42	1.48	1.65
4	1.98	0.94	1.43	1.53	1.71
5	2.11	0.88	1.44	1.56	1.88
6	2.14	0.93	1.47	1.61	1.93
7	2.16	0.92	1.48	1.62	1.90
8	2.21	0.98	1.48	1.66	1.91
9	2.22	0.98	1.51	1.68	2.13
10	2.27	0.99	1.52	1.71	2.42
11	2.30	1.01	1.53	1.73	2.53
12	2.37	1.01	1.57	1.74	2.52
13	2.41	1.03	1.58	1.75	2.71
14	2.44	1.04	1.62	1.78	2.77
15	2.51	1.05	1.63	1.82	2.69

The results pointed out in Fig. 10 and Table 2 clearly show that MVFT outperforms SVFT as well as other standard indoor localization algorithms, which testifies of the robustness and the feasibility of the proposal.

Nevertheless, the results also show that for one testdata, the triangulation technique outperforms the rest of the algorithms. Strictly speaking, such result cannot be fully discarded. This is mainly due to the fact that triangulation approach does not rely on the fingerprints but only on access points. On the other hand, it is almost unanimously acknowledged that any fingerprinting like approach is ultimately restricted by the density and homogeneity of the radio map created at the offline stage in the sense that the denser the radio map, the higher likely is the accuracy of the estimation.

Table 2 also shows a constant increase of the accuracy of all localization algorithms with respect to noise intensity, which is also trivially expected. On the other hand, it is worth pointing out that the variation of both MVFT and SVFT is relatively smaller than the variations of other algorithms, which demonstrates, to some extent, the robustness of the fuzzy inference system to noise. To see it, a graphical illustration is described in Fig 11. The graph restricts the plot to MVFT and kNN only for clarity of illustration.
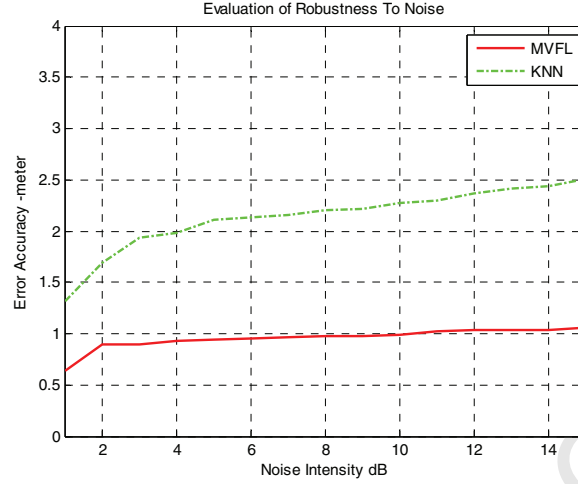
Fig 11 MVFL vs kNN robustness against noise

VII. Multivariable Fuzzy System Localisation with Outliering Augmentation

During the test phase of the program it was noticed that the multi-nearest neighbour algorithm (kNN) in many cases fails to locate the actual nearest fingerprints, due to uncertainty pervading the RSS value as well as the density of the fingerprint map, yielding sometimes inconsistent nearest neighbors. This obviously would affect any localization algorithm built upon the outcome of the initial KNN including the developed MVFL algorithm. It was noticed, for instance, from our simulation results, that to locate 4 nearest neighbor of 16 test-points the kNN fails on average of 16% to 19% locating the actual nearest neighbors in a testbed of 64 fingerprints distributed symmetrically over 20x20 meters space. To overcome this challenge, we introduced some robust ad-hoc rule aiming to outlier some of the misplaced nearest neighbors. Inspired from robust statistics [55], the proposed *outliering* algorithm relies on a distance based triangulation method, where the points elected by the kNN algorithm are considered only if the kNNs fingerprints tend to establish a *triangle* of a smallest area. This intuitively would discard those fingerprints which are spatially located far away from the closest neighbor, but, on the other hand, requires us to investigate those fingerprints that are close to the k-nearest neighbors in the signal space. More formally, the area of each possible triple combination of fingerprints is calculated using the following equation:

$$Area = \left| \frac{A_x(B_y - C_y) + B_x(A_y - C_y) + C_x(A_y - B_y)}{2} \right| \tag{28}$$

Where $\{A_x, B_x, C_x\}$ and $\{A_y, B_y, C_y\}$ are the x-coordinates and y-coordinates of the three corner points (fingerprints), respectively. The above process is therefore repeated for each triple in the set of 2K nearest neighbors while ensuring that at least one of the fingerprints of the k-nearest neighbors is included in the triple. This reasoning is motivated by the desire to introduce more flexibility in the choice of the nearest neighbors based only on RSS values by allowing for an extended range of neighbors up to 2K and accounting for spatial disposition of the fingerprints. The choice of 2K neighbors, where the search of candidate fingerprints is enabled, is only motivated by the computational cost. For instance, for K=3, the number of triples that will be search for will be $\sum_{i=1}^{2K-2} i + \sum_{i=1}^{2K-3} i + \sum_{i=1}^{2K-4} i = 19$.

Consequently, the number of triples to be searched increases drastically with the size of the neighbor region. A brief description of the above approach is summarized in Fig. 12.

Enhanced K-nearest Region
 FOR Each fingerprint in K-nearest region
  Pick up two distinct fingerprints in 2K-neighbor region
  Calculate Area of triangle using (27)
 END
  Select triple that yields smallest Area

Figure 12. Overview of Robust K-nearest selection

Especially, it has been observed during our simulation experiment that the use of such outliering scheme reduces the kNN failure to less than 5% from a previous 13% estimate.

Fig. 13 highlights the performance of the outliering K-NN scheme when compared to standard K-NN. The performance metric in this graph consists of the average positioning error (across all targets) with respect to the number of Monte Carlo simulation employed. Needless to say that the use of only KNN for positioning; namely, averaging across the three optimal fingerprints in the sense of area minimization provides only a rough indication on the quality of the newly obtained nearest neighbor that would be used as a basis for further localization algorithms. The graph shows clearly that the outliering kNN outperforms the standard kNN in this respect. Nevertheless, the augmented kNN algorithm may mark some fingerprints as outlier points while they might be the real nearest fingerprints, which justifies the occurrence of possible mismatch, which, in turn, influences the accuracy of the positioning algorithm. This partly explains the fact that sometimes standard kNN yields better result than outliering kNN.
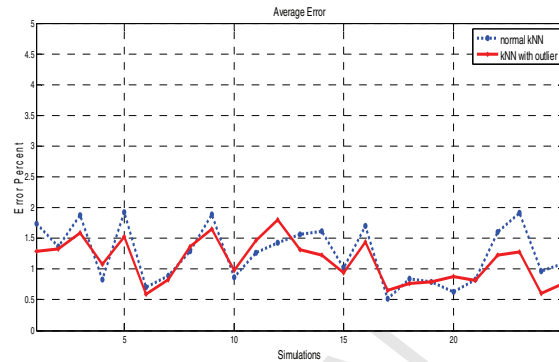

Figure 13. kNN vs. kNN with outlier

In order to test the performance of the outliering kNN, we compared the performances of the FMVL algorithm with outliering kNN and with standard kNN when using different noise intensities ranging from 0 to 15 dB. The results are summarized in Table 3.

Table 3. Error in location estimation of kNN vs augmented kNN with outlier stage

Noise S_{dB}	Average Accuracy Error	
	MVFL-kNN	MVFL-Robust kNN
1	0.4201	0.5301
2	0.4343	0.5742
3	0.5401	0.5756
4	0.5640	0.6102
5	0.7447	0.6214
6	0.9126	0.6344
7	1.1235	0.6816
8	1.2381	0.7156
9	1.5376	0.9782
10	1.8047	1.1635
11	2.2356	1.3166
12	2.9395	1.5714
13	3.0325	1.5844
14	3.0542	1.5936
15	3.2326	1.8617

As it can be seen in Table 3, the augmented kNN algorithm enhanced the performance of the localization algorithm especially when the intensity of noise becomes important.

Strictly speaking, when the noise is very small, the use of standard kNN algorithm is expected to perform better, which is also noticed in the first four tuples of Table 3. This is due to the fact that when noise is relatively small, the RSS values are still providing good estimate, therefore, there is less ambiguity in terms of which fingerprints will be associated with. While such ambiguity increases substantially as the noise intensity increases, which, in turn, decreases the accuracy of kNN-MVFL algorithm as it will fail to locate the nearest neighbors accurately.

This limitation opens room to enhance to the performance of the augmented kNN by investigating each individual case, especially when the target points are located somewhere outside the collected fingerprint space. One main idea can be via applying various distance measures, provide directional base outliering algorithm, and use the outliering to acquire knowledge about the certainty level of the localisation process or level of noise on RSS value in the environments. Some of these cases are still under investigation as part of our future works.

VIII. EXPERIMENT

In addition to the previous simulation study, an experimental case study at our laboratory has taken place. The experimental setup has been designed to be close enough to the simulation setup. The layout of the testbed is illustrated in Fig. 14, where a total of 40 fingerprints and 10 test-points were used. Four WX-1590 SparkLAN wireless multimode APs compatible IEEE 802.11b were installed close to the roof and corners. A pocket PC Compaq iPAC 3970 with network card Lucene Wi-Fi Orinoco Gold Card were used to store RSS data from APs. The room is about 20m x20m size. The average distance between two fingerprints is about 1.5m. Besides, some of the fingerprints were obstructed by a wall in the middle, in order to test the effect of NLOS.

During the offline stage, at each fingerprint, the signal strength is averaged over a time window of 5sec. The average RSS values at each fingerprint, with respect to each Access Point, together with the associated standard deviation, were reported. This process is also repeated when few persons (3-4 persons) randomly move inside the room. This is motivated by the desire to create more realistic scenarios for test cases where the measurement may likely involve human presence. On the other hand, the water present in human bodies as well as the orientation of the individuals have the physical property of absorbing signal strength, which, in turn, would affect the RSS values received from access point. Consequently, accounting for such fluctuation in the offline stage would undoubtfully enhance the credibility of the offline stage. More formally, the RSS value RSS_{ij} at i^{th} fingerprint from j^{th} access point will be calculated as

$$RSS_{ij} = \frac{\alpha.\overline{RSS_{ij}}^{\alpha} + \beta_1.\overline{RSS_{ij}}^{1} + \beta_2.\overline{RSS_{ij}}^{2} + ... + \beta_n.\overline{RSS_{ij}}^{N}}{\alpha + \beta_1 + \beta_2 + ... + \beta_N} \tag{29}$$

Where $\overline{RSS_{ij}}^{\alpha}$ stands for the mean value of RSS values (from i^{th} fingerprint to j^{th} access point) in situation of no individuals, except the operator, are present in the room, and α stands for the associated standard deviation. While $\overline{RSS_{ij}}^{k}$ (k= 1 to N) stands for the means of RSS value during the kth random movement of the individuals (random number between 1 to 4 individuals), with the associated standard deviation β_k. The accumulation of the RSS values collected as in (19) constitutes the radio map and offline stage of the localization process.
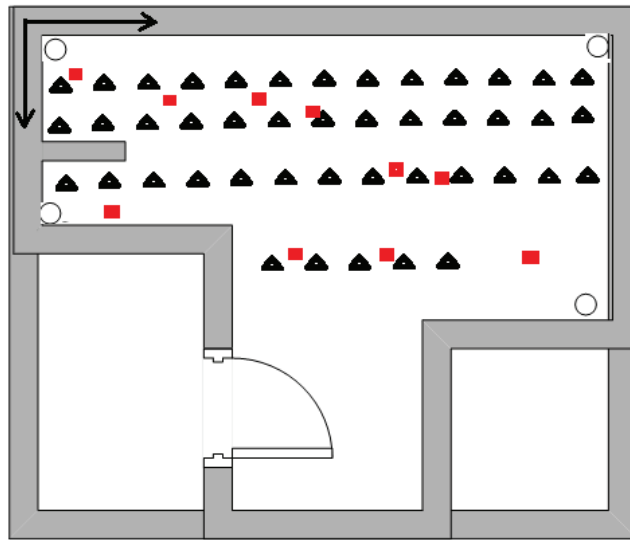

Figure 14. Experimental testbed

The coordinates of the various fingerprints and test-points were quantified in 3D Cartesian space as indicated in the graph. The 3D representation was justified by the APs placed on the roof, while the x-y plan was adjusted to be on the same level as the fingerprints and test-points yielding a $z=0$ component for those points.

The results of the various localizations algorithms are summarized in Table 4. The outcomes correspond to the localization error at each test-point.

Table 4 Error in location estimation using different localization algorithms

Test-Point	Average Accuracy Error				
	kNN	MVFL	SVFL	W-KNN	LAT
1	1.21	0.44	0.72	0.83	0.62
2	0.74	0.48	0.61	0.71	1.52
3	0.88	0.26	0.42	0.34	1.44
4	1.43	0.49	0.53	0.77	0.39
5	1.41	0.38	0.61	0.71	0.94
6	0.94	0.31	0.54	0.63	1.33
7	2.36	0.81	1.12	1.23	1.10
8	0.91	0.18	0.48	0.46	1.08
9	0.84	0.26	0.51	0.38	0.93
10	2.74	0.98	1.55	1.31	1.02

The results highlighted in Table 4 show clearly that the MVFL outperforms other localization algorithms in most cases. Although, one notices the following:
- The evaluation of the performance of the localization algorithm has been done on manual basis through mapping the point in the environment testbed and quantifying the squared mean error. Consequently, cautious should be taken in terms of the level of accuracy due to the difficulty of such visual mapping procedure.
- The organization of the test-points in the experimental design is such that it would likely yield some confusion scenarios.
- Indeed, some test-points were deliberately located very close to each other, e.g., fifth and sixth test-point. This would inevitably influence the accuracy of any positioning system as the signal strength values would yield close values.
- Some test-points were voluntary located relatively far from any fingerprints (e.g., seventh test-point). This again would trivially affect the quality of the fingerprinting based positioning algorithms, while, on the other hand, this would favour triangulation like algorithm as it does not rely on fingerprint. This explains the superiority of triangulation for such test-points.
- Due to presence of obstructing obstacles and the specific geometry of the room, signal from some access points may not be received by some test-point (e.g., 8th test-point). Similar situation also occurred during the offline stage. Nevertheless such cases have not influenced at all the performance and functioning of the localization algorithms, due to the fact that normalized distance (2) were used.
- The use of triangulation involves the use of radio propagation in the sense of (7). Although, results in Table 3 corresponding to triangulation make use of the mean value yield by (7); namely,

$$RSS = -40 - 31log_{10}(d), \tag{30}$$

one shall point out that it is also worth investigating the extreme cases. In other words, the process is repeated for both expressions:

$$RSS_1 = -40 - 31log_{10}(d) - 8 \tag{31}$$
$$RSS_2 = -40 - 31log_{10}(d) + 8 \tag{32}$$

This would yield an interval evaluation of the triangulation result where the true position would, at least theoretically, lie in. Nevertheless, in practice such expectation is not always met due to uncertainty pervading the data as well the triangulation approach itself. On the hand, looking at the range of RSS values in the experiment, which ranges from -88dB to -63dB, shows that this is in full agreement with radio propagation model (7). Indeed, without accounting for NLOS effect, which trivially increases the range of distances, putting the admissible fingerprint/test-point -AP- distances in the range 3m to 24m either in expression (7) or in Figure 3 yields signal strengths values from -46.8 dB to -90.8 dB. While the interval [-88dB -63dB] is trivially included in [-46.8dB -98.8dB].
- The overall positioning accuracy for the MVFL algorithm is around 43 cm, while some test-points achieved less than 20 cm accuracy and others slightly more than one meter. This also testifies on the high performance of the developed algorithm

given that such accuracy is only a fraction (around one third) of the average distance between two consecutive fingerprints. This fraction seems also to be in agreement with that of simulation results where almost same performance rate were achieved. The variability of the RSS signal always restricts the accuracy that can be obtained by any RSS-based localization approach.

- The algorithms employed in the experimental part have not used the outliering approach to refine the nearest neighbours. This is mainly due to the simulation results, which show that such approach is only interesting in case of increasing noise in the environment, otherwise, the performance may get degraded because we may end up averaging over inappropriate neighbours.

IX. CONCLUSION

This paper investigates a new approach for wireless indoor localization using fuzzy logic. The proposal is based on the refinement of k-nearest neighbor fingerprinting algorithm, where the weight attached to each nearest neighbor is determined using a Takagi-Sugeno fuzzy system. Two inputs were used to the fuzzy system. The first one corresponds to the distance in signal space from the test-point (target node) to each nearest neighbor. The second corresponds to the difference of the signal variations between the target and the nearest neighbor fingerprint. The performances of the proposal have been evaluated in both simulation and experimental settings and compared to several alternative approaches, including, triangulation, standard KNN, weighted KNN and single input variable fuzzy-based positioning already proposed in literature. The results demonstrated the feasibility of the proposal and its superiority in most scenarios. Some refinements of the proposal have also been put forward in order to handle the uncertainty pervading the RSS values. This includes robustification in the choice of nearest neighbors based on triangulation. Also, the choice of the membership functions has been refined to accommodate the radio propagation model and the observed fluctuations in terms of standard deviations of the RSS signals at various conditions, e.g., presence of absence of users in environment testbed. This work has opened new perspective work in terms of enhancing the nearest neighbor approach as well as the fuzzy inference system. Indeed, both the number of nearest neighbors and the distance metric expression can be questioned. Especially, since the signal strength values are non-uniformly distributed within their universe of discourse in the sense, for instance, that range of RSS values between -65dB and -80dB are much more dominant than other ranges, it will be interesting to design a metric that enhances such discrimination power. Similarly, enforcing some flexibility and adaptivity on the choice of K would reduce the amount of the associated uncertainty. On the other hand, the current fuzzy system calculates the weight associated to each nearest neighbor from the two inputs involving only the target node and the associated nearest fingerprint. This implicitly assumes full independence among the fingerprint measurements. However such assumption is not always valid. Indeed, for instance, all measurements do share the same target node. This makes the conditional independence a more plausible assumption rather than of full independence.

X. REFERENCES

[1] J.A. Castellanos and J.D. Tardos. *Mobile Robot Localization and Map Building: A Multisensor Fusion Approach*. Kluwer Academic Publishers, Boston, MA, 2000.

[2] E. Guizzo and T. Deyle, Robotics Trends for 2012. *IEEE Robotics and Automation Magazine,* Vol. 19, No. 1, 2012, 119-123.

[3] V. Kumar, 50 Years of Robotics, *Special Issue of IEEE Robotics and Automation Magazine* Vol. 17, No. 3, 2010.

[4] A. Kupper, Location Based Services: Fundamentals and Operation, John Wiley, 2005.

[5] T. D'Roza and G. Bilchev, An Overview of location based services, *BT Technology Journal*, Vol. 21, No.1, 2003, 20-27.

[6] Y. Gu, A. Lo and I. Niemegeers, A Survey of Indoor Positioning Systems for Wireless Personal Networks, *IEEE Communications Surveys and Tutorials*, Vol. 11(1), 2009, pp. 13-32.

[7] H. Liu, H. Darabi, P. Banerjee and J. Liu, Survey of wireless indoor positioning techniques and systems, *IEEE Transactions On Systems, Man, and Cybernetics—Part C: Applications And Reviews*, Vol. 37, No. 6, 2007, pp.1067-1080.

[8] T. S. Rappaport, *Wireless Communications Principles and Practice*, 2nd Edition, Prentice Hall Upper SaddleRiver, NJ, USA, 2001

[9] B. Li, Y. Wang, H. Lee, A. Dempster, and C. Rizos, Method for yielding a database of location fingerprints in WLAN, *Communications, IEE Proceedings-*, Vol. 152, no. 5, 2005, pp. 580–586.

[10] C. M. Bishop, *Machine Learning and Pattern Recognition*, Springer, Singapore, 2006.

[11] M. Alakhras, M. Oussalah and M. Hussein, Multivariable Fuzzy Inference with Multi Nearest Neighbour for Indoor WLAN Localization Based on RSS Fingerprint, *Proceedings of IEEE UKSIM'13 AMSS-15th International Conference on Modelling and Simulations,* Cambridge University, *2013*

[12] T. Takagi and M. Sugeno, Fuzzy identification of systems and its applications to modelling and control, *IEEE Transactions On Systems, Man, And Cybernetics*, Vol. 15, No. 1, 1985, pp. 116-132.

[13] P. Bahl and V. N. Padmanabhan, RADAR: An in-building RF-based user location and tracking system, Microsoft Research, *IEEE INFOCOM* 2000, pp. 775-784.

[14] P. Bahl and V. N. Padmanabhan and A. Balachandran, *Enhacements to the RADAR User Location and Tracking System*, Technical Report MSR-TR-2000-12, Microsoft Research, 2000.

[15] M. Youssef, A. Agrawala, and U. Shankar. WLAN Location Determination via Clustering and Probability Distributions. In *IEEE PerCom 2003*, March 2003.

[16] M. Brunato and C. K. Kallo, Transparent Location Fingerprinting for Wireless Services, in: *Proceedings of Med-Hoc-Net Conference*, Vol. 2002, 2002

[17] A. Kushki, K. Plataniotis, and A. Venetsanopoulos, Kernel-Based Positioning in Wireless Local Area Networks, *IEEE Transactions on Mobile Computing*, Vol. 6, No. 6, 2007, pp. 689-705.

[18] Y. Wang, X. Jia, H.K. Lee and G.Y. Li, An indoors wireless positioning system based on wireless local area network infrastructure, in: *Proceedings of the 6th International Symposium on Satellite Navigation Technology Including Mobile Positioning & Location Services*, Melbourne, Australia, 2003.

[19] R. Want, A. Hopper, V. Falcao, J. Gibbons, The Active Badge Location Systems, *ACM Transactions on Information Systems*, Vol 40, No.1, 1992, pp 91-102.

[20] T. D. Hodes, R. H. Katz, E. S. Schreiber, and L. Rowe, Composable Ad Hoc Mobile Services for Universal Interaction, in: *Proceedings of MobiCom '97 Conference*, 1997, pp: 1-12.

[21] H. Laitinen, J. Lahteenmaki, and T. Nordstrom. Database Correlation method for GSM location. In: *Proceedings of the 53rd IEEE Vehicular Technology Conference*, Rhodes, Greece, May 2001

[22] K. Laasonen, M. Raento, and H. Toivonen. Adaptive on-device location recognition. In: *Proceedings of the Second International Conference on Pervasive Computing*. Springer-Verlag, 2004, pp. 287–304.

[23] A. LaMarca, Y. Chawathe, S. Consolvo, J. Hightower, I. Smith, J. Scott, T. Sohn, J. Howard, J. Hughes, F. Potter, J. Tabert, P. Powledge, G. Borriello, and B. Schilit. Place Lab: Device Positioning Using Radio Beacons in the Wild. *Proceedings of 3rd Annual Conference on Pervasive Computing*, 2005.

[24] Ekahau, http://www.ekahau.com

[25] X. Li, Y. Chen, J. Yang and X. Zheng, Achieving Robust Wireless Localization Resilient to Signal Strength Attacks, *Wireless Networks*, Vol. 18, 2012, pp. 45-58.

[26] Shum, K.C.Y.; Quan Jia Cheng; Ng, J.K.Y.; Ng, D., A Signal Strength Based Location Estimation Algorithm within a Wireless Network, in: *Proceedings of the 2011 IEEE International Conference on Advanced Information Networking and Applications (AINA)*, 2011, pp.509-516.

[27] K. H. Lee, *First Course on Fuzzy Theory and Applications*, Advances in Soft Computing, Springer, 2005

[28] C. Y. Chen, J. P. Yang, G. J. Tseng, Y.H. Wu, and R. C. Hwang, An indoor positioning technique based on fuzzy logic, in: *Proceeding of the International Multi Conference of Engineers and Computer Scientists*, Vol. II, IMCES2010. Hong Kong 2010

[29] A. Teuber, B. Eissfeller, A two-stage fuzzy logic approach for wireless LAN indoor positioning, in: *Proccedings of IEEE/ION Position, Location and Navigation Symposium,* San Diego, CA, 2006, pp. 730-738

[30] A. Rozyyev, H. Hasbullah and F. Subhan, Combined k-nearest neighbors and fuzzy logic indoor localization technique for wireless sensor network, *Research Journal of Information Technology*, Vol. 4, 2012, pp. 155-165.

[31] M. Bshara, U. Orguner, F. Gustafsson and L. Van Biesen, Fingerprinting localization in wireless networks based on recieved-signal-strength measurements: A case study on WiMAX networks, *IEEE Transaction on Vehicular Technology*, Vol. 59, No. 1, 2010, pp. 283-295.

[32] S. Gansemer, U. Grobmann, S. Hakobyan, RSSI-based Euclidean distance algorithm for indoor positioning adapted for the use in dynamically changing WLAN environments and multi-level buildings, in: *Proceedings of the IEEE International Conference on Indoor Positioning and Indoor Navigation (IPIN)*, 2010.

[33] J. Hightower and G. Borriello, Location Systems for Ubiquitous Computing, *IEEE Computer Society Press*, Vol. 34, No. 8, 2001, pp. 57-66

[34] A. K. M. Mahtab Hossain, Yunye Jin, Wee-Seng Soh, Hien Nguyen Van: SSD: A Robust RF Location Fingerprint Addressing Mobile Devices' Heterogeneity. *IEEE Transaction on Mobile Computing* Vol. 12, No. 1, 2013, pp. 65-77.

[35] A. Shamir, An introduction to radio to radio waves propagation: generic terms and practical approached to path loss calculations, including examples, *Technical Report RFwaves LTD,* rev 1.0, 2002.

[36] B. F. Wu, C-L. Jen and K-C. Chang, Neural Fuzzy Based Indoor Localization by Kalman filtering with Propagation Channel Modelling, In: *Proceedings of the IEEE International Conference on Systems, Man and Cybernetics*, 2007 pp. 812-817.

[37] T. Bilgic and I. B. Turksen, Measurement of membership functions: theoretical and empirical work. In: *Fundamental of Fuzzy Sets, The Handbook of Fuzzy Sets Series*, Ed: D. Dubois and H. Prade, Vol. 7, 2000, pp.195-227.

[38] K. Kaemarungsi, P. Krishnamurthy, Properties of indoor received signal strength for WLAN location fingerprinting, in: *Proceedings of MOBIQUITOUS'04: First Annual ACM International Conference on Mobile and Ubiquitous Systems: Networking and Services*, Boston, MA, USA, 2004, pp. 14-23.

[39] P. P. Angelov, D. P. Filev, An approach to online identification of Takagi-Sugeno fuzzy models, IEEE Transactions on Systems, Mans and Cybernetics, Part B., 34(1), 2004, 484-498

[40] S. L. Chiu, Fuzzy model identification based on cluster estimation, J. of Intelligent Fuzzy Systems, 2, 1994, 267-278

[41] J. Q. Chen, Y. G. Xi and Z.J. Zhang, A clustering algorithm for fuzzy mode identification, Fuzzy Sets and Systems 98, 319-329.

[42] J.S. Roger Jang, Anfis: adaptive-network-based fuzzy inference system, IEEE Trans. Systems Man Cybernet. 23 (1993), 665–685.

[43] W. Pedrycz and M. Reformat, Evolutionary fuzzy modeling. IEEE Trans. Fuzzy Syst., 11 (5), 2003, 652-665

[44] L. Wang and J. Mendel, Generating fuzzy rules by learning from examples. IEEE Trans. On SMC **22** (1992) 1414–1427

[45] L. Wang, Adaptive Fuzzy Systems and Control: design and stability analysis. Prentice-Hall, New Jersey, 1994

[46] J. Yen, L. Wang, and Gillespie C. W., "Improving the interpretability of TSK fuzzy models by combining global learning and local learning", *IEEE Transactions on Fuzzy Systems*, vol. 6, no. 4, pp. 530–537, 1998.

[47] S. Nefti, M. Oussalah, Kaymak, Fuzzy Rulebase simplification by inclusion based clustering, IEEE Trans., Fuzzy Systems, 16(1), 2008,

[48] M. Cerrada, J. Atuilar, E. Colina and A. Titli, Dynamical membership functions: An approach for adaptive fuzzy modeling. Fuzzy Sets and Systems , 152, 2005, pp: 513-533.

[49] M. Männle, "FTSM — Fast Takagi-Sugeno Fuzzy Modeling", in *Proceedings of SAFEPROCESS 2000*, Budapest, 2000, pp. 663–668.

[50] S. Destrecke, S. Guillaume and B. Charnomordic, Building an interpretable fuzzy rule base from data using orthogonal least squares. Application to a depollution problem. Fuzzy Sets and Systems, 158, 2007, 2078-2094.

[51] Y. Shi, M. Mizumoto, Some considerations on conventional neuro-fuzzy learning algorithms by gradient descent method, Fuzzy Sets and Systems 112 (2000) 51–63.

[52] M. Sugeno and T. Yasukawa, A Fuzzy logic based approach to qualitative modelling, IEEE Transactions on Fuzzy Systems 1(1), 1993, 7-31.

[53] M. Riedmiller and H. Braun, "A direct adaptive method for faster backpropagation: the RPROP algorithm", in *Proceedings of the IEEE Int. Conf. on Neural Networks (ICNN)*, 1993, pp. 586–591.

[54] T. Johansen and B. Foss. Identification of non-linear system structure and parameters using regime decomposition. *Automatica* **31**(2), 1995, 321–326

[55] P. Huber, *Robust Statistics*, John Wileys and Sons, Vol 523 of Wiley Series in Probability and Statistics, NY, 2004

Appendix - Triangulation Localization

First, from the signal strength RSS$_{iT}$, one uses the model (18), which yields a distance $d_{iT} = 10^{\frac{-RSS_{iT}-40}{31}}$

From the system of equation

$$\begin{cases} (x_{AP_1} - x_T)^2 + (y_{AP_1} - y_T)^2 + (z_{AP_1} - z_T)^2 = R_{1T}^2 = 10^{\frac{-2(RSS_{i1}-40)}{31}} \\ (x_{AP_2} - x_T)^2 + (y_{AP_2} - y_T)^2 + (z_{AP_2} - z_T)^2 = R_{2T}^2 = 10^{\frac{-2(RSS_{2T}-40)}{31}} \\ . \qquad \qquad . \qquad \qquad . \\ (x_{AP_n} - x_T)^2 + (y_{AP_n} - y_T)^2 + (z_{AP_n} - z_T)^2 = R_{nT}^2 = 10^{\frac{-2(RSS_{nT}-40)}{31}} \end{cases}$$

Subtracting from equation (1) each of the subsequent equation in the above system yields, after some manipulations

$$\begin{cases} x_{AP_1}^2 - x_{AP_2}^2 + y_{AP_1}^2 - y_{AP_2}^2 + z_{AP_1}^2 - z_{AP_2}^2 - R_{1T}^2 + R_{2T}^2 = \\ \qquad 2(x_{AP_1} - x_{AP_2})x_T + 2(y_{AP_1} - y_{AP_2})y_T + 2(z_{AP_1} - z_{AP_2})z_T \\ x_{AP_1}^2 - x_{AP_3}^2 + y_{AP_1}^2 - y_{AP_3}^2 + z_{AP_1}^2 - z_{AP_3}^2 - R_{1T}^2 + R_{3T}^2 = \\ \qquad 2(x_{AP_1} - x_{AP_3})x_T + 2(y_{AP_1} - y_{AP_3})y_T + 2(z_{AP_1} - z_{AP_3})z_T \\ . \qquad \qquad . \qquad \qquad . \\ x_{AP_1}^2 - x_{AP_n}^2 + y_{AP_1}^2 - y_{AP_n}^2 + z_{AP_1}^2 - z_{AP_n}^2 - R_{1T}^2 + R_{nT}^2 = \\ \qquad 2(x_{AP_1} - x_{AP_n})x_T + 2(y_{AP_1} - y_{AP_n})y_T + 2(z_{AP_1} - z_{AP_n})z_T \end{cases}$$

Using matrix formulation this comes down to

$$A = \begin{bmatrix} 2(x_{AP_1} - x_{AP_2}) & 2(y_{AP_1} - y_{AP_2}) & 2(z_{AP_1} - z_{AP_2}) \\ 2(x_{AP_1} - x_{AP_3}) & 2(y_{AP_1} - y_{AP_3}) & 2(z_{AP_1} - z_{AP_3}) \\ . \\ 2(x_{AP_1} - x_{AP_n}) & 2(y_{AP_1} - y_{AP_n}) & 2(z_{AP_1} - z_{AP_n}) \end{bmatrix}$$

$$B = \begin{bmatrix} x_{AP_1}^2 + y_{AP_1}^2 + z_{AP_1}^2 - (x_{AP_2}^2 + y_{AP_2}^2 + z_{AP_2}^2) + R_{2T}^2 - R_{1T}^2 \\ x_{AP_1}^2 + y_{AP_1}^2 + z_{AP_1}^2 - (x_{AP_3}^2 + y_{AP_3}^2 + y_{AP_3}^2) + R_{3T}^2 - R_{1T}^2 \\ . \\ x_{AP_1}^2 + y_{AP_1}^2 + z_{AP_1}^2 - (x_{AP_n}^2 + y_{AP_n}^2 + z_{AP_n}^2) + R_{nT}^2 - R_{1T}^2 \end{bmatrix}$$

This can be written in matrix form as

$$A \begin{bmatrix} x_T \\ y_T \\ z_T \end{bmatrix} = B$$

So, the use of least square yields

$$\begin{bmatrix} x_T \\ y_T \\ z_T \end{bmatrix} = \left(A^T A\right)^{-1} \left(A^T B\right)$$